PHYSICAL REVIEW D VOLUME 11, NUMBER 8 15 APRIL 1975

# Calculation of asymptotic behavior of form factors in non-Abelian gauge theories*

James J. Carazzone,[†] Enrico C. Poggio, and Helen R. Quinn[‡]
*Lyman Laboratory of Physics, Harvard University, Cambridge, Massachusetts 02138*
(Received 18 December 1974; revised manuscript received 6 February 1975)

We calculate the leading contributions to the fermion–fermion–vector-meson form factor with non-Abelian gluons exchanged between the fermions in the region $-q^2 \gg p^2, p'^2 > m^2$, $q^2$ spacelike, to sixth order in perturbation theory. For either incoming photon or gluon we obtain a result which shows that these contributions do not add to give a simple form. This paper presents the calculation in detail.

## I. INTRODUCTION

We have studied the vector-meson–fermion–fermion vertex for non-Abelian gauge theories in the limit

$$-q^2 \gg p^2,\ p'^2 > m^2 \geqslant 0\,, \qquad (1.1)$$

where $q$, $p$, and $p'$ are as defined in Fig. 1 and $m$ is the fermion mass. We have calculated the leading contributions in this limit through sixth order in perturbation theory. We find that these give a form factor

$$F(q^2,p^2,p'^2) = 1 - Kx + \frac{(Kx)^2}{2!} - \frac{(Kx)^3}{3!} + \Delta_0\,, \qquad (1.2)$$

where

$$x = \frac{g^2}{8\pi^2}\ln\left(\frac{-q^2}{p^2}\right)\ln\left(\frac{-q^2}{p'^2}\right) \text{ and } \Delta_0 = \frac{-K'}{12}\,\frac{x^3}{3!}\,. \qquad (1.3)$$

The purpose of this paper is to discuss the details of the calculation.[1]

The constants $K$ and $K'$ in (1.2) depend on the nature of the incoming particle. More explicitly, our model includes any nontrivial group of massless vector fields interacting with themselves in the usual Yang-Mills fashion and coupled minimally to some multiplet of fermions via the matrix $T_a$, the generator of the gauge group in the fermion representation:

$$\mathcal{L} = -\tfrac{1}{4}F^a_{\mu\nu}F^{a\mu\nu} - \tfrac{1}{4}G_{\mu\nu}G^{\mu\nu} + \bar\psi\gamma_\mu(\partial_\mu - igB^a_\mu T_a - ieA_\mu)\psi - m\bar\psi\psi\,, \qquad (1.4)$$

where

$$F^a_{\mu\nu} = \partial_\mu B^a_\nu - \partial_\nu B^a_\mu + igf^{abc}B^b_\mu B^c_\nu\,,$$
$$G_{\mu\nu} = \partial_\mu A_\nu - \partial_\nu A_\mu\,, \qquad (1.5)$$

and

$$[T_a, T_b] = if_{abc}T_c\,. \qquad (1.6)$$

The incoming vector meson in Fig. 1 may be either a gauge group singlet $A$, in which case we shall refer to it as the photon, or a member of the nontrivial gauge multiplet $B$, in which case we call it a gluon. The fermions are gauge group nonsinglet (colored) elementary particles. Defining the Casimir operators of the gauge group by

$$C_N = T_aT_a \qquad (1.7)$$

and

$$C_AT_c = -if_{abc}T_aT_b\,, \qquad (1.8)$$

we find for an incoming photon

$$K = C_N,\quad K' = C_A^2C_N\,, \qquad (1.9)$$

while for a gluon

$$K = C_N - C_A,\quad K' = C_A^2(C_N - C_A)\,. \qquad (1.10)$$

Equation (1.2) can be restated as the observation that the leading contributions to the form factor in the region (1.1) to all orders in perturbation theory can be written as

$$F(q^2,p^2,p'^2) = e^{-Kx} + \Delta\,, \qquad (1.11)$$

where the leading contribution to $\Delta$ is $\Delta_0$.

The simple relationship between the photon and gluon results, $C_N \to (C_N - C_A)$, depends on the fact that only a certain class of diagrams contribute leading terms and on some subtle cancellations,

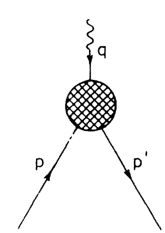


FIG. 1. The vertex function showing momentum labeling used throughout our discussion. The incoming vector meson is either a photon or a gluon.

in the gluon case, between contributions that depend on higher-order Casimir operators.

Before embarking on a discussion of the details of our calculation we would like to make some general comments about the motivation for performing it and the meaning of our result. We are interested in the general question of dynamics in a quark-gluon theory of strong interactions. As we shall show later the logarithms appearing in each order of perturbation theory in (1.2) are infrared or large-distance effects. If they do not sum to some simple damped contribution they will be a dominant feature of any calculation based on the notion of multiquark bound states.[2] For example, they could dominate over short-distance effects and hence, could possibly destroy naive scaling behavior for composite-particle scattering at wide angles and for composite-particle form factors.[3]

The implication of our result for these calculations requires further study. It is not clear whether the contribution of $\Delta$ or that of terms of lower order in $g^2$ which are nonleading logarithms will be more important in these calculations. We have not made any attempt to calculate nonleading logarithmic contributions.

As is the case for the Abelian theory the leading contributions to the vertex function in the limit (1.1) come from the low-momentum end of loop integrations. Ultraviolet singularities generate, at most, one power of a logarithm for each loop integration. These can be handled with some off-mass-shell renormalization procedure. The details of this procedure are of no concern to us because the leading terms as $q^2 \to \infty$ are ultraviolet finite and thus not affected by the subtractions. As $p^2$, $p'^2$, and $m^2 \to 0$ the vertex function becomes infrared singular in such a way that one obtains two powers of $\ln q^2$ for each loop integration from certain diagrams. In the Abelian theory these diagrams are just ladders and crossed ladders. We shall show that through sixth order in perturbation theory in the non-Abelian case one obtains such contributions from all possible diagrams in which a complex of gluons is exchanged between the two fermion lines and these gluons interact among themselves only through trigluon couplings. We speculate that this result will continue to apply in higher orders. It is sufficient to keep $p^2$ and $p'^2$ finite and set $m^2 = 0$ to obtain an infrared-finite result. We make all our calculations in this limit. Introducing a nonzero fermion mass will only alter nonleading terms.

The organization of this paper is as follows: In Sec. II we show that the graphs which may contribute leading logarithmic terms are the same for an incoming gluon as for an incoming photon, and in Sec. III we discuss the group-theoretic weights in the two cases. Section IV gives details of the fourth-order calculation, Sec. IV B being devoted to the new features of the non-Abelian case. In Sec. V we discuss the sixth-order calculation and Sec. VI makes some concluding comments. There are two appendixes. Appendix A presents an alternate discussion to that of Sec. IV B, which gives a concise evaluation of certain graphs. Appendix B contains a detailed calculation of the sixth-order graph given in Fig. 12(a), thus presenting an explicit application of the methods discussed in Sec. V.

## II. COMPARISON OF INCOMING GLUON AND PHOTON

If the incoming meson is a gauge group singlet (such as the photon in a color gauge theory), it does not interact with the non-Abelian gluons. Thus, the vertex-function diagrams in this case all have the incoming hard vector meson attached directly to the fermion line. However, if the incoming particle is itself a gluon (one of the vector mesons transforming according to the adjoint representation of the gauge group), it can couple to the fermion line directly, but it can also be attached to other vector lines or ghost loops via its non-Abelian interactions, as in the diagrams of Fig. 2. We find that all such diagrams are infrared finite for $p^2$ and $p'^2 \to 0$ and hence, do not generate any leading contributions in the region of interest (1.1). This is important for the simplicity of our result, as it means that the diagrams which do give leading contributions are the same for incoming photons and for gluons.

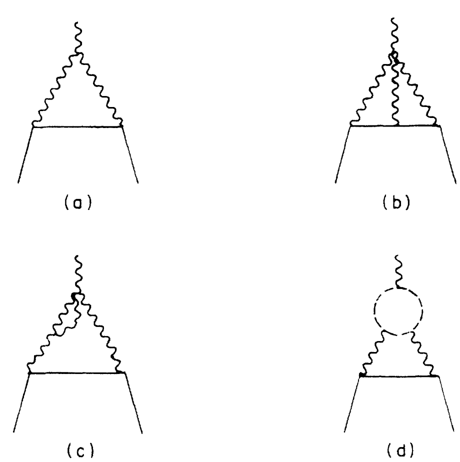


FIG. 2. Diagrams particular to the case when the incoming vector meson is a gluon. They are infrared infinite and thus do not contribute leading logs.

Let us first examine the diagram of Fig. 2(a). One can readily convince oneself that, for any choice of momentum routing, this diagram behaves at worst like $\int d^4k/k^3$ for $k\to 0$, and $p^2=p'^2=0$. Simple power-counting arguments show that one cannot make a diagram which is infrared divergent in every subintegration by adding lines to this diagram.[4] This argument includes additions which convert the three-point coupling into a four-point coupling [such as Fig. 2(b) and 2(c)], as the infrared finiteness of Fig. 2(a) is not dependent on the numerator factors in the Yang-Mills three-point coupling.

This leaves only diagrams such as Fig. 2(d) where the incoming gluon attaches to a ghost loop. Figure 2(d) itself is also clearly infrared finite because of the numerator factor of loop momentum in the ghost loop. Thus, any higher-order diagram where the incoming gluon is attached to a ghost loop is also infrared finite.

This being so, the only difference between the calculation for an incoming photon and that for an incoming gluon is that the gluon connects to the fermion with a group matrix $T_a$, whereas for the photon the corresponding factor is 1. This means that each diagram contributes with a different group-theoretic weight in the two cases. We will next determine the relationship between these weight factors for all the graphs which give leading logarithmic corrections. Because of some subtle cancellations the total weights (sum of all the weights) through sixth order are simply related.

## III. GROUP-THEORETIC WEIGHTS

The group-theoretic weight of each diagram can be written in terms of the Casimir operators of the group. At each gluon-fermion vertex there is a group matrix $T_a$ and at each Yang-Mills vertex a structure function $f_{abc}$. We define the quantities $C_N$, $C_A$, and $H$ by

$$T_a T_a = C_N\,, \tag{3.1a}$$

$$if_{abc} T_a T_b = -C_A T_c\,, \tag{3.1b}$$

$$if_{axy}\, if_{byz}\, if_{czw}\, if_{dwx}\, T_a T_b T_c = H T_d\,. \tag{3.1c}$$

These defintions also imply that

$$if_{axy}\, if_{byz}\, if_{czx} = -C_A\, if_{abc} \tag{3.2}$$

and

$$T_a T_b T_a = (C_N - C_A) T_b\,. \tag{3.3}$$

The weight of each graph can then be obtained by commuting the $T$ matrices of the fermion numerator and applying (3.1) and (3.2). The higher-order Casimir operator $H$ does not enter the photon calculation through sixth order in perturbation theory. The weight for any $2n$th-order photon graph can thus be written as a sum of terms of the form $C_A{}^{n-m}P_m$ where

$$P_m = T_{a_1}\cdots T_{a_m}\underline{1}\,T_{a_m}\cdots T_{a_1} = C_N{}^m\,. \tag{3.4}$$

For an incoming gluon the $\underline{1}$ in (3.4) is replaced by $T_\theta$, where $\theta$ is the group index carried by the hard gluon. This replaces each factor $C_N$ by a factor $C_N - C_A$. In addition, some graphs have contributions which vanish for an incoming photon but which involve the higher-order Casimir operator $H$ for an incoming gluon.[5] We will denote such contributions by $F$, where $F=0$ for an incoming photon and $F=H-C_A{}^3$ for an incoming gluon. In our subsequent discussion we will give all weights for the case of an incoming photon, though keeping track of the possible $F$ contributions. The gluon result is then obtained by making the substitution $C_N \to C_N - C_A$ and $F=H-C_A{}^3$ in the given expressions.

## IV. FOURTH-ORDER CALCULATION OF THE VERTEX

### A. Ladder and crossed-ladder graphs

The lowest-order contribution to the photon-fermion-fermion vertex is identical to the lowest-order QED diagram multiplied by an overall factor of $C_N$. In QED the evaluation of the leading contributions to the vertex function in the limit (1.1) was performed to all orders in perturbation theory by Sudakov,[6] who used a convenient momentum-space method. It was found that the leading contributions in each order of perturbation theory were given by the sum of ladder and crossed-ladder diagrams. The leading contribution from each of these diagrams was shown to arise from the low-momentum portion of the loop integrations, using the routing shown in Fig. 3, and was com-

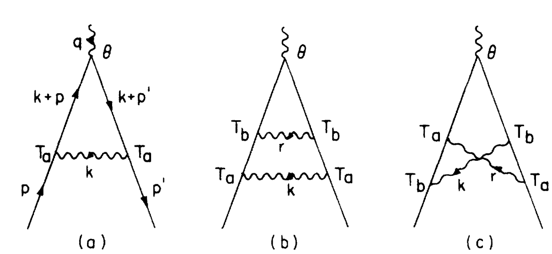


FIG. 3. (a) Second-order diagram showing choice of internal momentum routing and group-theoretic labeling. $\theta$ can either be 1 or $T_b$. (b) Fourth-order ladder graph. (c) Fourth-order crossed-ladder graph.

puted to be

$$\frac{1}{(n!)^2}\left[\frac{-g^2}{8\pi^2}\ln\left(\frac{p^2}{-q^2}\right)\ln\left(\frac{p'^2}{-q^2}\right)\right]^n \tag{4.1}$$

for each of the $(n!)$ contributing diagrams in $2n$th-order perturbation theory. The sum of the leading contributions in each order therefore takes on decaying exponential form,

$$\Gamma(p,p')\sim e^{-x}, \tag{4.2}$$

with

$$x=\frac{g^2}{8\pi^2}\ln\left(\frac{p^2}{-q^2}\right)\ln\left(\frac{p'^2}{-q^2}\right). \tag{4.3}$$

The contribution of order $g^2$ is given by Fig. 3(a) for both the Abelian and non-Abelian theories. The only difference is that in the non-Abelian case it enters with a group-theoretic weight factor coming from the gluon-fermion vertices. For an incoming photon the contribution is

$$A_2=-C_N x. \tag{4.4}$$

In fourth order in the Abelian case the diagrams of Fig. 3(b) and 3(c) each contribute $(1/2!)^2x^2$. In the non-Abelian theory they enter with different group-theoretic weight factors. For Fig. 3(b) the weight is $T_aT_bT_bT_a=C_N^2$ and for Fig. 3(c) the corresponding factor is $T_aT_bT_aT_b=C_N(C_N-C_A)$. Thus, the sum of these two contributions gives

$$A_4(\text{ladder}+\text{crossed ladder})=\frac{2C_N^2-C_NC_A}{(2!)^2}x^2. \tag{4.5}$$

This is clearly not the next term in an expansion of an exponential (or any other simple function) that begins with $(1-C_Nx)$.

### B. Non-Abelian contribution

The non-Abelian aspects of our model theory provide us with diagrams not found in QED, and we shall see that the extra leading terms generated by these diagrams just cancel the term of Eq. (4.5) due to the non-Abelian algebra. We find that Fig. 4(a) contains a leading contribution. To discuss this it is convenient to first summarize some of the features of the three-propagator Feynman integral

$$I_3=\int\frac{d^4k}{(2\pi)^4}\,\frac{1}{(k+p_1)^2(k+p_2)^2(k+p_3)^2}. \tag{4.6}$$

This integral has been analyzed in detail by Sudakov.[6] Using the usual Feynman parametrization, and defining $\Delta_{ij}=(p_i-p_j)^2$ we find

$$I_3=\frac{i}{(4\pi)^2}\int d\alpha_1\int d\alpha_2 \times\int d\alpha_3\,\frac{\delta(1-\alpha_1-\alpha_2-\alpha_3)}{\alpha_1\alpha_2\Delta_{12}+\alpha_1\alpha_3\Delta_{13}+\alpha_2\alpha_3\Delta_{23}}. \tag{4.7}$$

Obviously, if for some choice $k$, $\Delta_{ik}=\Delta_{jk}=0$ this integral is doubly logarithmically divergent. Thus, if for any choice $p_i,p_j,p_k$ are such that

$$-\Delta_{ij}\gg\Delta_{ik},\Delta_{jk}>0, \tag{4.8}$$

then in this region

$$I_3=\frac{i}{(4\pi)^2}\,\frac{1}{\Delta_{ij}}\ln\left|\frac{\Delta_{ik}}{\Delta_{ij}}\right|\ln\left|\frac{\Delta_{jk}}{\Delta_{ij}}\right|. \tag{4.9}$$

The double logarithm arises from the region of momentum space $k+p_k\to 0$ and corresponds to the infrared singularity of the integral when $\Delta_{ik}=\Delta_{jk}=0$. In general, there are three possible contributions of the form of (4.9) corresponding to different regions of the momenta external to this loop. When the integration is internal to some other loop integrations we need only keep those contributions which allow the remaining integrations to become singular. Any terms for which there are conflicts between the constraint (4.9) for successive integrations will not contribute leading logarithms. It is also useful to note that the constraint (4.9) is not satisfied for any choice $i,j,k$ for a loop with a repeated denominator.

We can now examine the contribution of Fig. 4(a). We route the momenta as shown in the diagram. The leading logarithmic contribution then

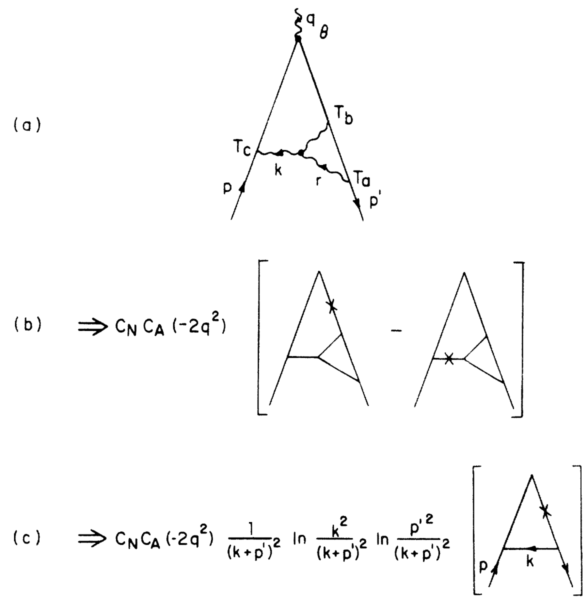


FIG. 4. (a) Fourth-order diagram with characteristic non-Abelian coupling. The dot at the three-gluon vertex represents a factor $if_{abc}$. (b) Reduction of diagram (a) to a $\varphi^3$ diagram. The $\times$ on a propagator denotes that propagator has been canceled by numerator factors. (c) Leading contribution from diagram (a) after integration of the Yang-Mills insertion.

comes from $k_\mu \to 0$ and $r_\mu \to 0$ so we can drop these terms relative to the external momenta $p$ and $p'$ in fermion numerators. We also drop any numerator terms proportional to $p^2$ or $p'^2$ as they will yield contributions suppressed by $p^2/q^2$ in the region (1.1). We retain denominator factors of $p^2$ and $p'^2$ as these provide the infrared cutoff. The contribution of Fig. 4(a) is then

$$D_{4(a)} = \int \frac{d^4k}{(2\pi)^4} \int \frac{d^4r}{(2\pi)^4} \frac{g^4 N_\sigma}{(p+k)^2(p'+k)^2 k^2 r^2 (r+p')^2(p+r)^2}, \tag{4.10}$$

where

$$N_\sigma = [(if_{abc}T_aT_bT_c)(\gamma_\rho \not{p}'\gamma_\nu \not{p}'\gamma_\sigma \not{p}\gamma_\mu)][(2r-k)^\mu g^{\nu\rho} - (r+k)^\nu g^{\mu\rho} + (2k-r)^\rho g^{\nu\mu}]. \tag{4.11}$$

Using the fact that this numerator stands between projection operators for the external (virtual) particles we can simplify it by commuting factors of $p'$ to the left and $p$ to the right, keeping only the terms which would survive for $p^2$ and $p'^2 \to 0$. We also simplify the group operators using (3.3). This gives

$$N_\sigma = C_N C_A (\underline{1}\gamma_\sigma)(4p\cdot p')2p'\cdot(k-2r) + O(p^2, p'^2). \tag{4.12}$$

The term proportional to $r$ in this numerator can also be dropped as it will give an infrared-finite contribution. Thus, finally we have

$$D_{4(a)} = C_N C_A g^4 (\underline{1}\gamma_\sigma)(-2q^2) \int \frac{d^4k}{(2\pi)^8} \left[\frac{1}{k^2(p+k)^2} - \frac{1}{(p'+k)^2(p+k)^2}\right] \int d^4r \frac{1}{r^2(r-k)^2(r+p')^2}. \tag{4.13}$$

This is represented diagrammatically in Fig. 4(b), where a $\times$ on a propagator indicates that the propagator has been canceled by a numerator term. We now perform the $r$ integration using the method discussed above to identify leading logarithms. The term corresponding to $\Delta_{ij} = (p'+k)^2$ in (4.9) is the only one which is consistent with the fact that the $k$-loop integration must give us two powers of logarithms in the region (1.1). This piece only contributes for the first term of the square bracket in (4.13):

$$\begin{aligned} D_{4(a)} &= C_N C_A g_n (\underline{1}\gamma_\sigma)(-2q^2) \int \frac{d^4k}{(2\pi)^4} \frac{1}{k^2(p+k)^2(p'+k)^2} \ln\left|\frac{p'^2}{(p'+k)^2}\right| \ln\left|\frac{k^2}{(p'+k)^2}\right| \\ &= C_N C_A g (\underline{1}\gamma_\sigma)(-2q^2) I, \end{aligned} \tag{4.14}$$

subject to the constraint

$$-(p'+k)^2 \gg k^2, p'^2.$$

To complete the evaluation of $D_{4(a)}$ we introduce Feynman parameters $\alpha_1$, $\alpha_2$, and $\alpha_3$ and define $k'_\mu$ by

$$k'_\mu = (k_\mu - \alpha_1 p_\mu - \alpha_2 p'_\mu) \tag{4.15}$$

to obtain

$$I = (2!) \int_0^1 d\alpha_1 d\alpha_2 d\alpha_3 \int \frac{d^4k'}{(2\pi)^4} \frac{\delta(1-\alpha_1-\alpha_4-\alpha_3)}{(k'^2 + q^2\alpha_1\alpha_2 + p^2\alpha_1\alpha_3 + p'^2\alpha_2\alpha_3)^3} \ln\left(\frac{-\Delta_1(k')}{p'^2}\right) \ln\left(\frac{-\Delta_1(k')}{\Delta_2(k)}\right), \tag{4.16}$$

where

$$\begin{aligned} \Delta_1(k') &= \{k'^2 + \alpha_1(1-\alpha_2)q^2 + 2k'\cdot[p\alpha_1 - p'(1-\alpha_2)] - \alpha_1\alpha_3 p^2 + (1-\alpha_2)\alpha_3 p'^2\}, \\ \Delta_2(k') &= k'^2 - \alpha_1\alpha_2 q^2 + 2k'\cdot(\alpha_1 p + \alpha_2 p') + \alpha_1^2 p^2 + \alpha_2^2 p'^2. \end{aligned} \tag{4.17}$$

The logarithms are slowly varying functions of $k'_\mu$, and to extract the leading logarithms we can make an approximation for the $k'_\mu$ integral of the form

$$\int dx \frac{1}{(x-a)^3} f(x) \approx \int dx \frac{1}{(x-a)^3} f(a), \tag{4.18}$$

provided $f(x)$ is sufficiently well behaved over the domain of integration. Thus,

$$I \approx \left(\frac{i}{(4\pi)^2}\right) \int_0^1 d\alpha_1 d\alpha_2 d\alpha_3 \delta(1-\alpha_1-\alpha_2-\alpha_3) \frac{1}{(q^2\alpha_1\alpha_2 + p^2\alpha_1\alpha_3 + p'^2\alpha_2\alpha_3)} \ln\left(\frac{-\Delta_1(s)}{p'^2}\right) \ln\left(\frac{-\Delta_1(s)}{\Delta_2(k_0)}\right), \tag{4.19}$$

where $s_\mu$ obeys

$$-s^2 = q^2\alpha_1\alpha_2 + p^2\alpha_1\alpha_3 + p'^2\alpha_2\alpha_3 .$$

We are interested in evaluating $I$ in the limit $p^2/(-q^2)\to 0$ and $p'^2/(-q^2)\to 0$. The leading contribution comes from the region where the denominator

$$D = (q^2\alpha_1\alpha_2 + p^2\alpha_1\alpha_3 + p'^2\alpha_2\alpha_3) \tag{4.20}$$

is near zero. This means that $s^2$ is near zero, and that $\alpha_1$ and $\alpha_2$ are small compared to one. We take $\alpha_3$ as nearly one. Over the domain

$$\omega' \equiv \frac{-p'^2}{q^2} \ll \alpha_1 \ll 1 ,$$
$$\omega \equiv \frac{-p^2}{q^2} \ll \alpha_2 \ll 1 , \tag{4.21}$$

we approximate $D$ by $(q^2\alpha_1\alpha_2)$ and $\Delta_1$ and $\Delta_2$ by

$$\Delta_1 \sim \alpha_1 q^2 ,$$
$$\Delta_2 \sim -\alpha_1\alpha_2 q^2 . \tag{4.22}$$

The integral now becomes

$$I \sim (i/4\pi)^2 \int_{\omega'}^1 d\alpha_1 \int_{\omega}^1 d\alpha_2 \frac{1}{q^2\alpha_1\alpha_2} \ln\left(\frac{-\alpha_1 q^2}{p'^2}\right) \ln\left(\frac{1}{\alpha_2}\right), \tag{4.23}$$

$$I \sim \frac{i}{(4\pi)^2}\frac{1}{(2!)^2}\frac{1}{q^2}\ln^2\omega\,\ln^2\omega' .$$

(An alternate derivation of this result is given in Appendix B.) Thus, the contribution of Fig. 4(a) is

$$D_{(4a)} = \frac{1}{2}\frac{C_N C_A x^2}{(2!)^2} , \tag{4.24}$$

when $x$ is defined in (4.3). The left-right reflected diagram yields an equal leading contribution.

Figure 5 shows all the remaining new diagrams in fourth order for the non-Abelian theory compared with the Abelian case. They all involve self-energy insertions and hence do not give leading logarithms. Thus, the total contribution in fourth order is

$$A_4 = \frac{x^2}{(2!)^2}[(2C_N^2 - C_N C_A) + (\tfrac{1}{2}C_N C_A)2]$$
$$= \frac{C_N^2 x^2}{2!} \tag{4.25}$$

and the sum of all leading logarithms up to fourth order yields

$$1 - C_N x + \frac{C_N^2 x^2}{2!} . \tag{4.26}$$

## V. SIXTH-ORDER CALCULATION

### A. General method of calculation

We wish to isolate graphs which yield a factor $(\ln q^2)^2$ for each loop integration. From the Abelian case we know that such terms are present for all ladder and crossed-ladder graphs. Straightforward iteration of the technique discussed in Sec. IV B will clearly yield such terms also for a generalized ladder or crossed-ladder graph in which any "rung" decomposes via trigluon couplings into a shower of gluons which join the fermion lines without further crossings.

Generalizing this technique, as we will describe, we find that the only leading contributions through sixth order are of the type shown in Fig. 6, where

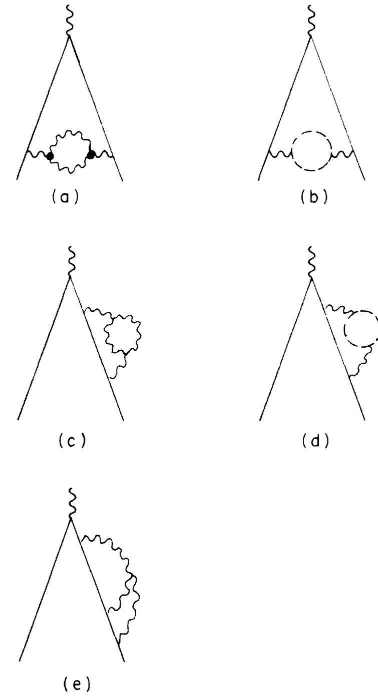


FIG. 5. New graphs in fourth-order non-Abelian theory which do not give leading logarithmic contributions.

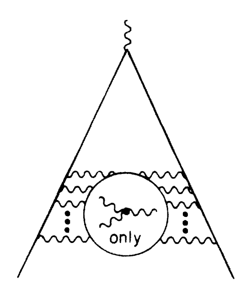


FIG. 6. Schematic representation of the class of diagrams which generate leading contributions. The blob represents all possible graphs where the gluons interact through trigluon couplings, including disconnected graphs.

the fermion lines exchange a set of gluons which interact among themselves through trigluon couplings only. This feature is essential for the simplicity of our result, and we believe that it will persist in higher orders. We will return to discuss this point further after a presentation of our calculational technique.

We can make an analysis similar to that of Sec. IV B for loops involving four propagators. If there is a numerator factor involving one or two powers of loop momentum we rewrite it as a sum of squares. The integrals with numerators which cancel one of the denominator terms are then evaluated in the usual way. The remaining terms are evaluated by selecting all possible sets of the denominators and Feynman parametrizing these. The remaining denominator in each term is then set equal to the value it has when the cubic denominator vanishes and the integration is performed. That is, we use the approximation (4.18) to evaluate each term. Since the terms correspond to different regions in momentum space one can obtain a leading contribution from one or more of them after subsequent integrations. Once again it is very important to check for the consistency of the imposed momentum constraints, in a sequence of integrations, to correctly isolate leading logarithms. The numerator factors of fermion propagators also restrict the possible choices of vanishing $\alpha$ parameters. We have checked that this method gives the correct result for a number of diagrams which we can also evaluate using only three-propagator loop integrations. It is very simple to use and quite unambiguous, provided the momentum constraints are correctly treated. In Appendix B we will carry out in detailed form the calculation of graph 12(a), where the above technique must be applied.

With these tools in hand we can now analyze a general diagram. We notice that the infrared singularities of a general vertex graph in the region $-q^2 \gg p^2$, $p'^2 > 0$ arise when the momentum $q$ does not flow through any line of the graph. By the arguments of Sec. II we are interested only in graphs where the incoming hard vector meson is attached to the fermion lines. In this way the infrared singularities are manifest, corresponding to internal momenta $k \to 0$. The internal gluon lines are all soft compared to fermion lines in the region of interest, and gluon momenta can be neglected in all fermion numerators. We arrange our numerator factors to cancel denominators whenever possible. We then integrate loop by loop. We always begin with the loop containing the smallest number of denominators, and use the approximation of (4.18) to simplify the arguments of the logarithms arising from previous loop integrations. The momentum constraints (4.8) from previous integrations are important. Whenever the constraints from two successive integrations are incompatible, the contribution from that term is nonleading. This technique allows us to evaluate all sixth-order diagrams. In higher orders one must eventually arrive at skeleton graphs where the simplest loop contains five or more propagators with numerator factors. Our method can probably be generalized to treat such cases.

### B. Graph-by-graph comments

The sixth-order graphs involving only trigluon couplings among exchanged gluons are shown in Figs. 7–12. We will now comment briefly on the calculation of each of these. We express our results for each graph as weights which are the coefficients of $-[1/(3!)^2]x^3$.

The ladder and crossed-ladder graphs of Fig. 7 are evaluated as for the Abelian theory. Using the group-theoretic properties and the definitions given in Sec. III we find the weights shown in Fig. 7 for each diagram. The sum of the ladder and crossed-ladder weights gives

$$6C_N{}^3 - 9C_N{}^2 C_A + 4C_N C_A{}^2 + 3F . \tag{5.1}$$

The graphs of Fig. 8 yield the contributions shown. The analysis of Fig. 8(a) is given in detail in Fig. 9. Numerator factors of the loop momen-

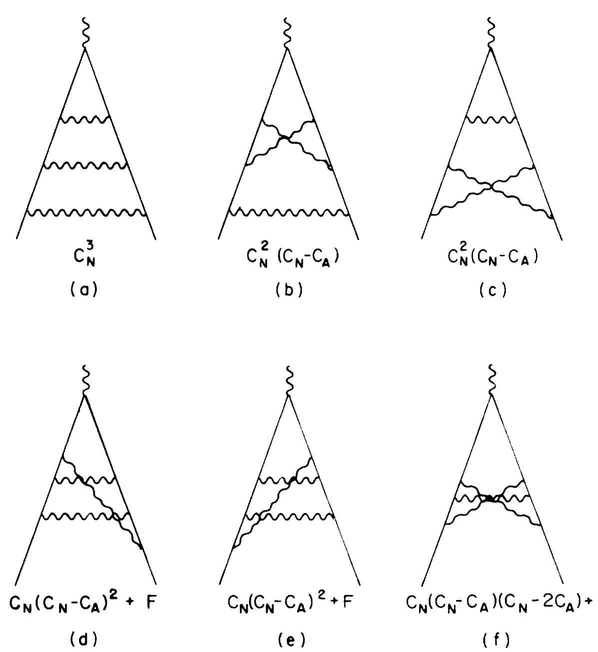


FIG. 7. Ladder and crossed-ladder contributions in sixth order. The weights shown are the coefficients of $-x^3/(3!)^2$.

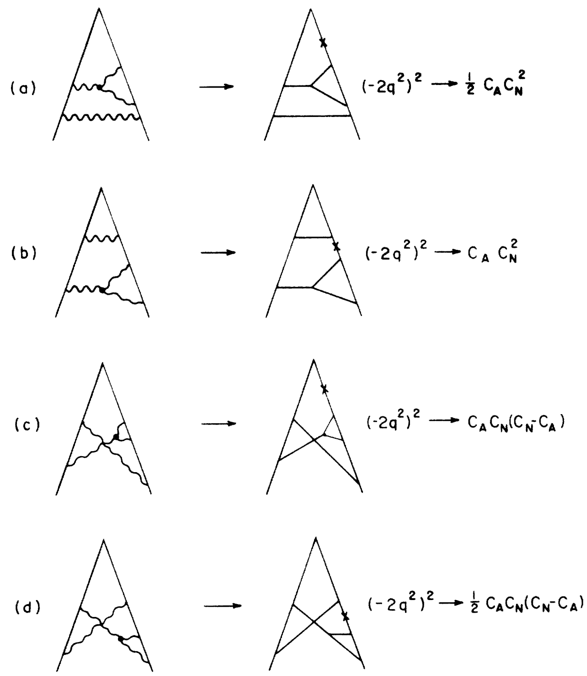


FIG. 8. Single-vertex insertion graphs in order and the corresponding dominant term after reduction to $\phi^3$ form.

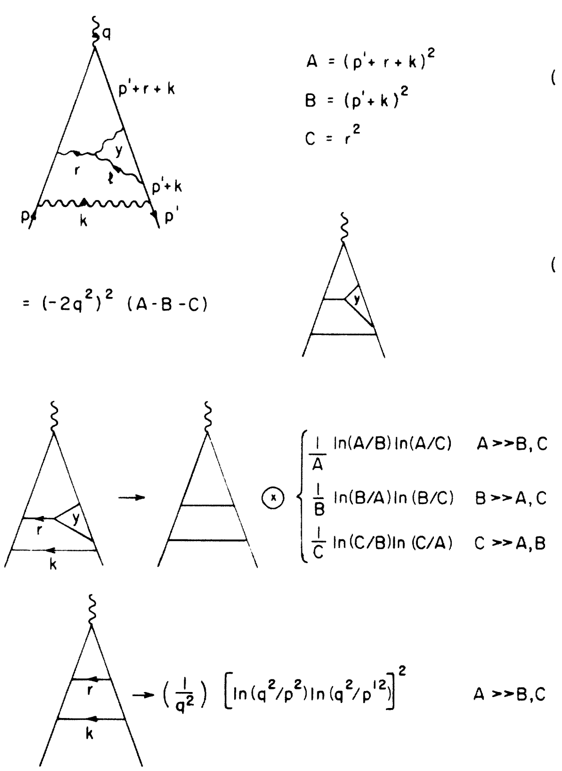


FIG. 9. Detailed analysis of Fig. 8(a).

tum $l$ can be dropped, as can any loop momenta in the numerators of fermion propagators. The resulting expression yields the contribution shown in Fig. 9(b). [For comparison note that each ladder graph can similarly be rewritten as $(-2q^2)^3$ times the corresponding ladder graph in a scalar $\phi^3$ theory.] The Yang-Mills insertion is next integrated. It contributes leading logarithms in three regions of momentum space, as listed in Fig. 9(c). The only leading logarithms arise where the factor $1/A^2$ from the integration of the insertion cancels the term $A^2$ in the numerator of Fig. 9(b). All other terms either have repeated denominators or are restricted to a region of momentum space for which the two-loop ladder graph does not yield leading logarithms. The procedure for the remaining graphs of Fig. 8 is identical. The significant terms are shown schematically in the figure, where $\times$ on a propagator means that the propagator has been canceled by a numerator term. The left-right reversed graphs yield identical leading logarithmic contributions. The graphs of Fig. 10 are similarly evaluated; again the contributions of left-right reversed graphs

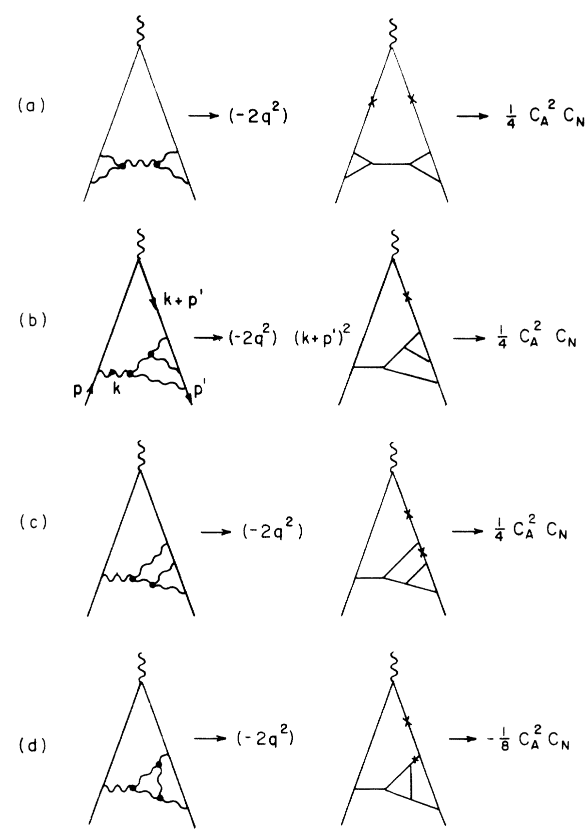


FIG. 10. Remaining generalized ladder graphs in sixth order.

are identical for leading logarithms.

We apply the same procedure for Fig. 11. Here there is no insertion but there is in each case at least one three-denominator loop after the cancellation of numerator terms. We perform such a loop integration first, which yields then a familiar two-loop form multiplied by two powers of logarithms. The remaining steps are as usual.

Figure 12 shows the graphs for which we are forced to evaluate four-propagator loops to obtain a result. These graphs also contain a new dynamical feature, for they involve 2-gluon–2-gluon scattering. Routing momenta as shown and neglecting the gluon momenta in fermion propagator numerators as usual, we find that the numerator of the integral to be evaluated for these graphs is

$$4q^4[k^2+s^2+(k-r)^2+(s-r)^2-(s-k)^2-2r^2]$$

$$-8q^2[3k\cdot p'r\cdot p+3r\cdot p's\cdot p-6k\cdot p'k\cdot p-6s\cdot p's\cdot p]$$

$$+\text{terms proportional to fermion masses.} \tag{5.2}$$

We find that the leading logarithmic contributions from the $q^4$ term cancel for both graphs of Fig. 12. The leading terms for Fig. 12(a) are the

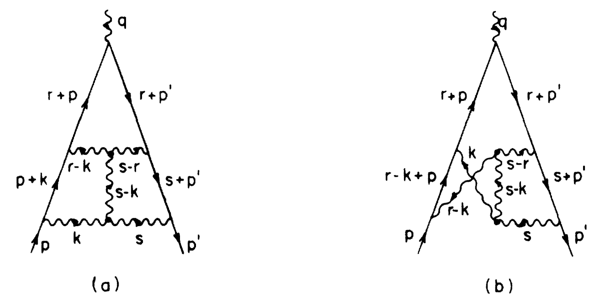


FIG. 12. The "$H$" graph and the "crossed $H$" graph showing a convenient momentum routing.

terms $k\cdot p'r\cdot p$ and $r\cdot p's\cdot p$. These give equal contributions of $\frac{3}{4}(C_NC_A^{\,2}+F)$. The remaining two terms do not give leading logarithms. To evaluate the contribution of Fig. 12(b) it is convenient to rearrange the $q^2$ term of (5.3) somewhat by adding and subtracting terms; for example,

$$3k\cdot p'r\cdot p-6k\cdot p'k\cdot p=-3k\cdot p'r\cdot p$$
$$+6k\cdot p'(r-k)\cdot p\,.$$

The second term on the right is nonleading and the first gives $-\frac{3}{2}F$. Similarly,

$$3r\cdot p's\cdot p=-3(r-s)\cdot p\,r\cdot p'+3r\cdot p\,r\cdot p'\,,$$

where the first term on the right gives $-\frac{3}{2}F$ and the second gives $+\frac{3}{2}F$. This gives the weights shown in Fig. 12. The evaluation of these graphs is given in detail in Appendix B. The graphs of Fig. 13 vanish identically. This follows from the group algebra [Eqs. (3.3) and (3.4)]. Finally, adding together all the sixth-order contributions, we find a cumulative weight

$$\frac{-C_N^{\,3}x^3}{3!}-\frac{1}{12}C_NC_A^{\,2}\frac{x^3}{3!}\,. \tag{5.3}$$

The complete set of our results is summarized in Fig. 14.

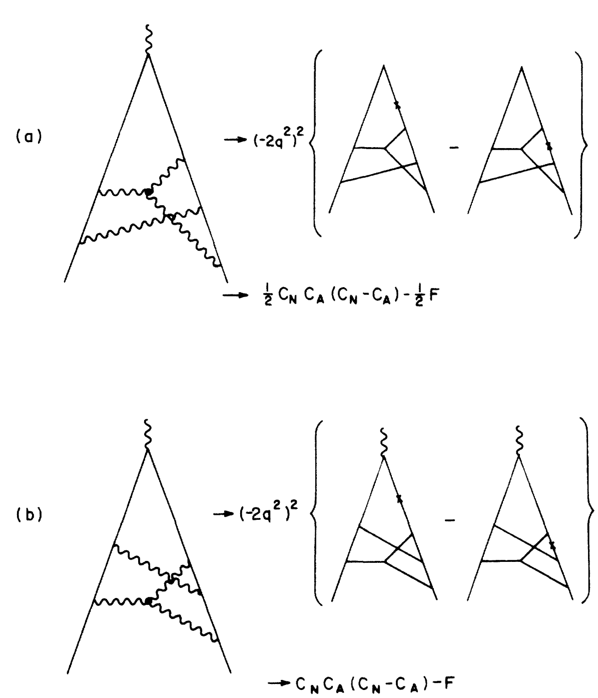


FIG. 11. Remaining nonplanar graphs with a single Yang-Mills vertex which contribute leading logarithms in sixth order.

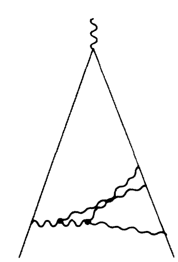

FIG. 13. Example of graph which is identically zero by group theory.

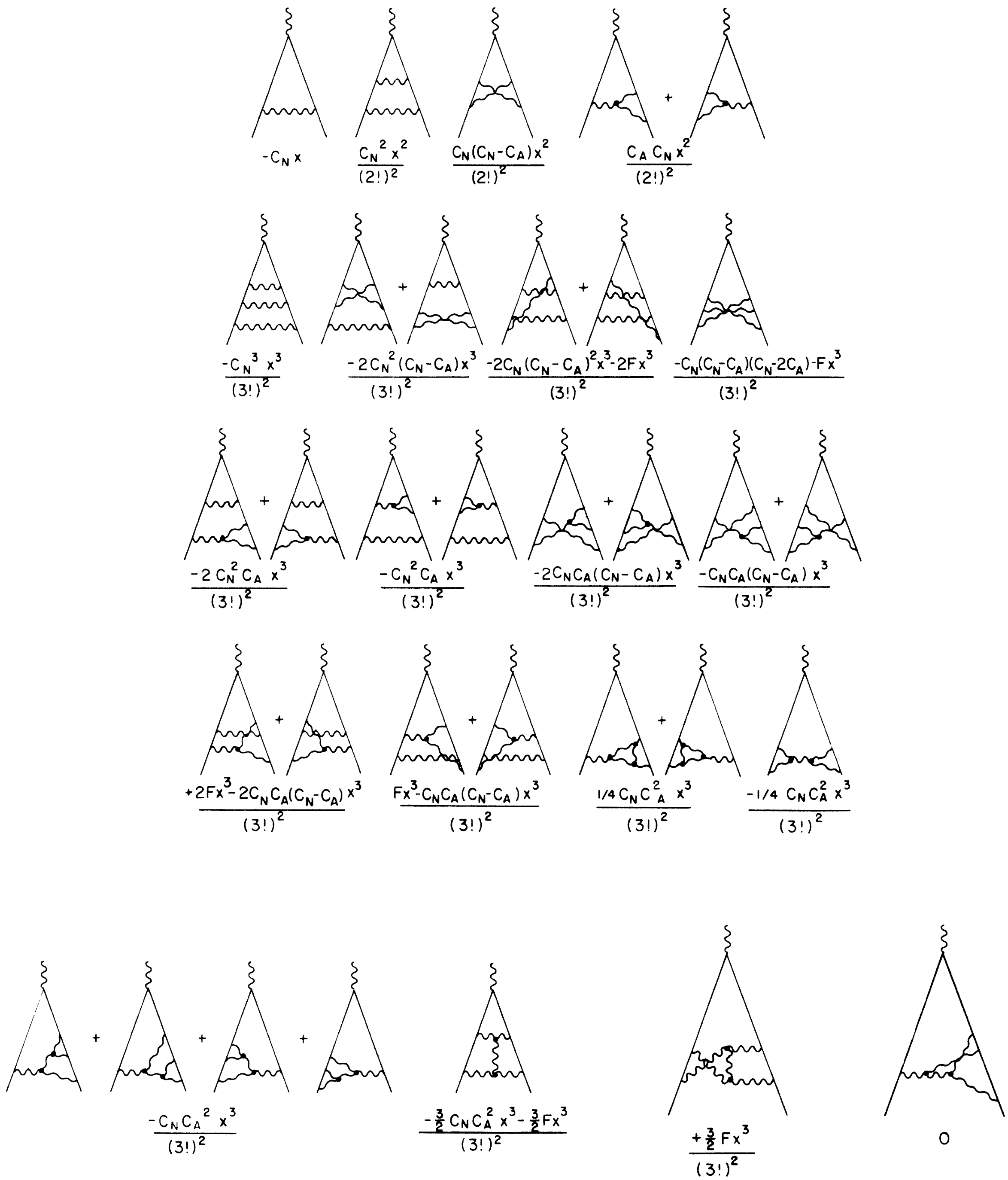


FIG. 14. Summary of the leading logarithmic contributions to the photon-fermion form factor through sixth order in perturbation theory. The quantity

$$x=\frac{g^2}{8\pi^2}\ln\left(\frac{-q^2}{p^2}\right)\ln\left(\frac{-q^2}{p'^2}\right).$$

Graphs with identical contributions are added together. For the gluon case $C_N \rightarrow (C_N - C_A)$ and $F \rightarrow (H - C_A^3)$.

### C. Nonleading contributions

We claim that the set of graphs which we have just discussed is all those which give leading contributions to this order. The remaining graphs can be subdivided into the following: (i) self-energy corrections on any line and/or graphs which appear in the Abelian theory and are known to be nonleading there, and (ii) new features in non-Abelian theory. Clearly we need not discuss the first case further, since they do not give leading logarithms. The new sixth-order graphs of class (ii) are shown in Fig. 15. Examination of Figs. 15(a) and 15(b) proceeds following our usual method, performing the insertion integration first. In each case there is at least one integration of the form of Fig. 16, when $r$ and $k$ are soft (in some cases $r\equiv 0$). This does not meet the requirement of Eq. (4.6) for the production of a double logarithm; it gives only a single logarithm. Hence, these graphs are nonleading.

The graphs of Figs. 15(c) and 15(d) which contain four-gluon couplings can be similarly evaluated. Integrating first loop $A$ and then loop $B$ we obtain four powers of logarithms. The final integration is a two-propagator loop in the case of Fig. 15(c) and a four-propagator loop with at least one repeated denominator for 15(d). Neither of these gives two powers of logarithms, so these graphs are nonleading.

The graph of Fig. 15(e) is infrared finite because of numerator factors in the ghost loop.

This completes our examination of all sixth-order contributions.

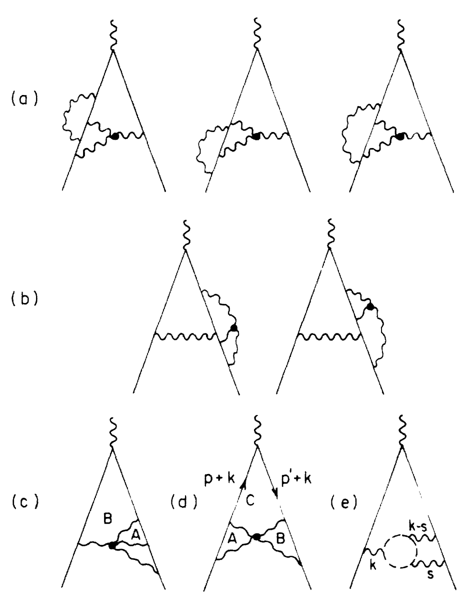


FIG. 15. Sixth-order graphs which do not generate leading logarithms.

### VI. COMMENTS AND CONCLUSIONS

Our principal result, Eq. (1.2), is gauge invariant and thus, unique. It should be further stressed that not only is the sum of leading logarithms gauge invariant, but also the leading logarithmic contribution of each graph is gauge independent.

We have carried out our calculations in the Feynman gauge, so that the vector-meson propagator is

$$D^{ab}_{\mu\nu}(k) = -i\delta^{ab}\frac{g_{\mu\nu}}{k^2}\ . \tag{6.1}$$

By adding to the propagator (6.1) a gauge piece $\lambda k_\mu k_\nu/k^4$ we find that contributions proportional to powers of $\lambda$ are all nonleading. This can readily be seen by remembering that three- or four-propagator loop integrations with repeated denominators do not give leading logarithms. Replacing $g_{\mu\nu}/k^2$ by $k_\mu k_\nu/k^4$ for any vector line leads to contributions with a repeated denominator and numerators which cancel some other denominator(s).

The remarkable feature of the fourth-order calculation is that all dependence on the Casimir operator $C_A$ cancels away in the photon case. If the exponential sequence were to continue in sixth order this feature would have to be maintained. That this does not occur seems to be the consequence of the new dynamical feature appearing in sixth order, namely the appearance of the gluon-gluon scattering contributions of Fig. 12. Similarly, the cancellation of the higher-order Casimir operator $H$ in the sixth-order gluon calculation is probably also a special case. In view of our result regarding $C_A$, we have no reason to believe that the cancellation will survive in higher orders. Eventually, even higher-order operators will start appearing.

Our result is true for all $p^2, p'^2 > m^2$. We have already seen that in this off-mass-shell case we can take $m^2 \to 0$ without any singularities. Singularities do arise if we try to put the external fermions on the mass shell.[7] Arbitarily introducing a gluon mass $\mu$ to cut off this singularity, we again obtain, through fourth order, the form of

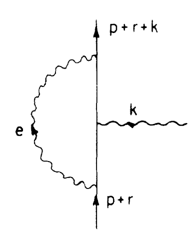


FIG. 16. Dressing of a single fermion line showing momentum routing.

(4.26) with now

$$x = + \frac{g^2}{16\pi^2}\left(\ln\frac{q^2}{\mu^2}\right)^2 . \tag{6.2}$$

We note that the gluon mass can be produced by the usual spontaneously broken symmetry method. The additional graphs involving scalar fields give contributions suppressed by powers of $q^2$.

The result of (1.2) cannot be checked or generalized by the renormalization-group approach.[8] The logarithms in (1.2) are of infrared origin and are independent of any choice of renormalization point or scale parameter. One cannot use scale-invariance arguments to obtain information about quantities which are functions of scale-invariant ratios such as $q^2/p^2$.

We conclude by remarking that the intermeshing of group-theoretic and dynamical features seen in this calculation will be a feature of any calculation in non-Abelian gauge theories.

*Note added in proof.* We have extended the calculation of the *on-mass-shell* fermion form factor to sixth order. We find that exponentiation fails by terms proportional to $C_N{}^2C_A$ and $C_NC_A{}^2$.


### ACKNOWLEDGMENTS

We would like to thank T. W. Appelquist and T. T. Wu for valuable discussions. One of us (E. C. P.) would like to thank the Aspen Center for Physics, where part of this work was carried out, for its congenial atmosphere and warm hospitality.


### APPENDIX A: EVALUATION OF CERTAIN FEYNMAN INTEGRALS

Here, we will analyze a certain class of Feynman integrals which occur in the evaluation of generalized ladder diagrams.

We are interested in calculating

$$I_N = \int \frac{d^4k}{k^2(k+P_1)^2(k+P_2)^2}\ln^N\left(\frac{k^2}{(k+P_i)^2}\right), \quad P_i = P_1, P_2 . \tag{A1}$$

Let us recall that

$$I_0 \sim \int \frac{d\alpha_1 d\alpha_2 d\alpha_3\,\delta(1-\alpha_1-\alpha_2-\alpha_3)}{(P_1-P_2)^2\alpha_1\alpha_2 + P_1{}^2\alpha_1\alpha_3 + P_2{}^2\alpha_2\alpha_3} . \tag{A2}$$

Using the following simple spectral form for the logarithm

$$\ln\left(\frac{k^2}{k_0{}^2}\right) = \int_0^\infty dM^2\left(\frac{1}{M^2+k_0{}^2} - \frac{1}{M^2+k^2}\right) \tag{A3}$$

we find that

$$\int \frac{d^4k}{k^2(k+P_1)^2(k+P^2)^2}\ln\left(\frac{k^2}{k_0{}^2}\right) \sim \int \frac{d\alpha_1 d\alpha_2 d\alpha_3}{D} \times \ln\left(\frac{D}{\alpha_3 k_0{}^2}\right), \tag{A4}$$

where

$$D = \alpha_1\alpha_2(P_1-P_2)^2 + \alpha_1\alpha_3 P_1{}^2 + \alpha_2\alpha_3 P_2{}^2 . \tag{A5}$$

A simple induction argument shows that

$$I_N = \int \frac{d^4k}{k^2(k+P_1)^2(k+P_2)^2}\ln^N\left(\frac{k^2}{k_0{}^2}\right) \sim \int \frac{d\alpha_1 d\alpha_2 d\alpha_3}{D}\ln^N\left(\frac{D}{\alpha_3 k_0{}^2}\right) . \tag{A6}$$

In particular, in the region $-(P_1-P_2)^2 \gg P_1{}^2, P_2{}^2$ we have

$$J_N \sim \frac{1}{(P_1-P_2)^2}\int_{\omega_1}^1 \frac{d\alpha_1}{\alpha_1}\int_{\omega_2}^1 \frac{d\alpha}{\alpha_2}\ln^N\left(\frac{q^2}{k_0{}^2}\alpha_1\alpha_2\right), \tag{A7}$$

where

$$\omega_i = \frac{P_i{}^2}{(P_1-P_2)^2} .$$

Similarly, it can be shown that

$$H_N = \int \frac{d^4k}{k^2(k+P_1)^2(k+P_2)^2}\ln^N\left(\frac{(k+P_i)^2}{k_0{}^2}\right) \sim \int \frac{d\alpha_1 d\alpha_2 d\alpha_3}{D}\ln^N\left(\frac{D}{k_0{}^2\alpha_i}\right), \tag{A8}$$

with the same $D$ as in (A5), and $\alpha_i = \alpha_1$ or $\alpha_2$ depending on whether $P_i = P_1$ or $P_2$. In the region $-(P_1-P_2)^2 \gg P_1{}^2, P_0{}^2$ we then have

$$H_N \sim \frac{1}{(P-P_2)^2}\int_{\omega_1}\frac{d\alpha_1}{\alpha_1}\int_{\omega_2}\frac{d\alpha_2}{\alpha_2}\ln^N\left[\frac{q^2}{k_0{}^2}\left(\frac{\alpha_1\alpha_2}{a_i}\right)\right] . \tag{A9}$$

Furthermore, integrals of the form $I_N$, as in (A1), will be

$$I_N \sim \int \frac{d\alpha_1 d\alpha_2 d\alpha_3}{D}\ln^N(\alpha_i) . \tag{A10}$$

From (A8) and (A10) one can further obtain formulas for integrals of the type

$$I_{N_1,N_2} = \int \frac{d^4k}{k^2(k+P_1)^2(k+P_2)^2}\ln^{N_1}\left(\frac{k^2}{(k+P_i)^2}\right) \times \ln^{N_2}\left(\frac{k^2}{P_i{}^2}\right) \sim \int \frac{d\alpha_1 d\alpha_2 d\alpha_3}{D^2}\,\delta(1-\alpha_1-\alpha_2-\alpha_3)\ln^{N_1}(\alpha_i) \times \ln^{N_2}\left(\frac{q^2}{P_i{}^2}\alpha_1\alpha_2\right), \quad i=1,2,\ j=1,2. \tag{A11}$$

As an example, we use these formulas to calculate diagram $D_{4a}$. From Sec. IV, we recall that the relevant integral is

$$I_{4a} \sim q^2 \int \frac{d^4k}{k^2(k+p)^2(k+P')^2} \ln\frac{(k+P')^2}{k^2} \ln\frac{(k+P')^2}{P'^2} . \tag{A12}$$

Using (B11) we obtain

$$I_{4a} \sim \int \frac{d\alpha_1}{\alpha_1} \int \frac{d\alpha_2}{\alpha_2} \ln\left(\frac{-q^2\alpha_2}{-q^2\alpha_1\alpha_2}\right) \ln\left(\frac{-q^2\alpha_2}{P'^2}\right), \tag{A13}$$

which is exactly the integral of (4.23) obtained by our general approximation method.

## APPENDIX B: EVALUATION OF DIAGRAM 12(a)

In order to amplify our discussion in Sec. V of the evaluation of four-propagator loop integrals, we will present here a fairly detailed computation of the diagram in Fig. 12(a). This diagram and that in Fig. 12(b) are the only ones that cannot be completely reduced down to the three-propagator loop integrals, or generalized ladders.

Using the momentum routing shown in Fig. 12, we find that the relevant numerator is

$$\begin{aligned} N = {} & 2^4(p\cdot p')^2[(k+s)\cdot(k+s-2r)] \\ & + 2^4(p\cdot p')[3(r\cdot p)(k\cdot p') + 3(s\cdot p)(+r\cdot p') \\ & - 6(k\cdot p)(k\cdot p') - 6(s\cdot p)(s\cdot p')] . \end{aligned} \tag{B1}$$

Let us first concentrate on the term proportional to $(p\cdot p')^2$. It can be rewritten as

$$k^2 + s^2 + (k-s)^2 + [(k-r)^2 - r^2] + [(s-r)^2 - r^2] .$$

The first three pieces cancel equal factors in the denominator and the three-propagator integrals thus produced yield nonleading logs. By the symmetry properties of the graph ($k \leftrightarrow -s$, $r \leftrightarrow -r$, $p' \leftrightarrow -p$) the two brackets will give identical contributions. We now examine the first of these.

The term $(k-r)^2$ cancels a term in the denominator and the resulting integral corresponds to the one of Fig. 8(b).

$$\int \frac{d^4k\, d^4r\, d^4s}{k^2(k-s)^2(k+p)^2(r-s)^2(r+p)^2(r+p')^2 s^2(s+p')^2} \to \frac{2}{(3!)^2} \ln^3 w \ln^3 w' , \tag{B2}$$

where $w = -p^2/q^2$ and $w' = p'^2/q^2$. The term $r^2$ does not cancel any denominator and thus the relevant integral contains at least four denominators (in every integration loop). The relevant integral is

$$J = \int \frac{d^4r\, d^4k\, d^4s\, r^2}{(r+p)^2(r+p')^2(r-k)^2(k+p)^2(k-s)^2(s^2)(s+p')^2(s-r)^2} . \tag{B3}$$

We perform the $s$ integration first. Define

$$J_{kr} = \int \frac{d^4s}{s^2(s-r)^2(s-k)^2(s+p')^2} . \tag{B4}$$

We observe that if we are to obtain a leading contribution, then $J_{kr}$ must integrate to give denominators of the form $1/r^2(k+p')^2$. Any other behavior will result in doubling existing denominators, and thus, yield nonleading contributions. With this in mind, we reduce (B4) into a three-denominators integral by using (4.18). In order to obtain all possible regions in $r$ and $k$ space which could give leading behavior, (4.18) must be applied by letting the function $f(s)$ be each of the four denominators in turn. Let us analyze each case separately:

(a) $f(s) = 1/s^2$.
Integral (B4) becomes

$$J_{kr}^{(a)} \to \int \frac{dx_1 dx_2 dx_3 \delta(1-x_1-x_2-x_3)}{[(k+p')^2 x_1 x_2 + (r+p')^2 x_1 x_3 + (r-k)^2 x_2 x_3][r x_3 + k x_2 - p' x_1]^2} . \tag{B5}$$

To get the desired behavior, we must have $x_1$ and $x_2$ approaching zero and $x_3$ approaching one. This corresponds to the region $s \to r$. The integral in (B5) becomes

$$J_{kr}^{(a)} \to \frac{1}{r^2(k+p')^2} \ln\frac{(r+p')^2}{(k+p')^2} \ln\frac{(r-k)^2}{(k+p')^2} , \tag{B6}$$

subject to the constraints $(p+p')^2(k-r)^2 < r^2(k+p')^2$, $(r+p)^2 < (k+p')^2$, $(r-k)^2 < (k+p')^2$. The first of these comes from the second denominator in (B5), the others from the first denominator in the usual way. The integral in (B3) is now of the three-denominators-per-loop form and one can proceed to see whether a leading contribution can be obtained. Doing the $r$ integration first, we obtain for it

$$\frac{1}{q^2}\int_{\sigma_1}\frac{dx_1}{x_1}\int_{\sigma_2}\frac{dx_2}{x_2}\ln\frac{q^2x_1}{(k+p')^2}\ln\frac{q^2x_1x_2}{(k+p')^2}\,,$$

$$r\to k-x_1p-x_2p'\,,$$

where

$$x_1>\sigma_1=\frac{(k+p')^2}{q^2}\text{ and }x_2>\sigma_2=\frac{(k+p)^2}{q^2}\,.$$

We thus observe that the constraint $(r+p')^2 < (k+p')^2$ is inconsistent with the constraint on $x_1$. Attempting to perform the $k$ integration first gives similar results. We conclude that the region region $s\to r$ does not give leading logs.

(b) $f(s)=1/(s-r)^2$.

We proceed as before. The region we are exploring now is $s\to 0$. The $s$ integral becomes

$$J_{kr}^{(b)}\to\frac{1}{r^2(k+p')^2}\ln\frac{k^2}{(k+p')^2}\ln\frac{p'^2}{(+p')^2}\,,$$

subject to the constraints $k^2<(k+p')^2$, $p'^2<(k+p')^2$, $k^2(r-k)^2<r^2(k+p')^2$, and $p'^2(r+p')^2<r^2(k+p')^2$. The remaining integral is now of the form corresponding to Fig. 8(b). All the constraints can be satisfied in obtaining the resulting leading contribution. This is exactly equal to that from the $(k-r)^2$ term given in (B2). Examining similarly the terms with $f(s)=1/(s-k)^2$ and $f(s)=1/(s+p')^2$ we find these give no leading logarithmic contributions. We thus conclude that the term proportional to $(p\cdot p')^2$ is nonleading.

The part proportional to $(p\cdot p')$ in (B1) can be easily evaluated by the three-denominator method to give the result of Fig. 14.

A similar analysis is carried out for Fig. 12(b). There the term proportional to $(p\cdot p')^2$ is analogously seen to give no leading log as in the previous discussion. The discussion of the term proportional to $(p\cdot p')$ is different since it involves, again, four-denominator integrals. We find the evaluation proceeds most simply by performing the $r$ integration first.

---

*Work supported in part by the NSF under Grant No. GP 40397X.

†Present address: Fermi National Accelerator Laboratory, P. O. Box 500, Batavia, Illinois 60016.

‡Alfred Sloan Foundation Fellow.

[1]See also James Carazzone, Ph.D. thesis, Harvard University, 1974 (unpublished).

[2]T. W. Appelquist and E. C. Poggio, Phys. Rev. D 10, 3280 (1974).

[3]S. J. Brodsky and G. Farrar, Phys. Rev. Lett. 31, 1153 (1973); Phys. Rev. D 11, 1309 (1975); V. A. Matveev, R. M. Muradyan, and A. N. Tavkhelidze, Nuovo Cimento Lett. 5, 907 (1972); 7, 719 (1973).

[4]As further illustration of this point is a theorem proved in Appendix A of Ref. 2.

[5]We thank Dr. R. Cahalan and Dr. D. Knight for pointing out an error in the group-theoretical discussion of a previous version of this paper, where the discussion of the Casimir operator $H$ was not taken into account.

[6]V. V. Sudakov, Zh. Eksp. Teor. Fiz. 30, 87 (1956) [Sov. Phys.—JETP 3, 65 (1956)]. This calculation can also be done simply using our general method described in Sec. V. For a different approach see V. Z. Blank, Dokl. Akad. Nauk USSR 107, 389 (1956) [Sov. Phys.—Dokl. 1, 184 (1956)].

[7]In the Abelian case, the on-mass-shell leading logarithm exponentiation (which is equivalent to an eikonal approximation) has been proven to all orders by T. W. Appelquist and J. Primack, Phys. Rev. D 4, 2444 (1971). This was originally suggested by R. Jackiw, Ann. Phys. (N.Y.) 48, 292 (1968).

[8]We thus disagree with the claims of N. N. Bogoliubov and D. V. Shirkov, in *Introduction to the Theory of Quantized Fields* (Interscience, New York, 1959). We would like to thank T. W. Appelquist for fruitful discussions on this generally misunderstood point.